Charge Carrier Dynamics of Standard TiO_2 Catalysts Revealed by Femtosecond Diffuse Reflectance Spectroscopy

Akihiro Furube,[†] Tsuyoshi Asahi,[†] Hiroshi Masuhara,*[,†] Hiromi Yamashita,[‡] and Masakazu Anpo[‡]

Department of Applied Physics, Osaka University, Suita, Osaka 565−0871, and Department of Applied Chemistry, College of Engineering, University of Osaka Prefecture, Gakuen-cho 1-1, Sakai, Osaka 599-8531

Received: October 26, 1998; In Final Form: February 5, 1999

Dynamics of charge carriers generated by femtosecond UV (160 fs, 390 nm) excitation in five standard TiO_2 photocatalytic powders (JRC-TIO-1, -2, -3, -4, and -5 supplied by the Catalysis Society of Japan) in a vacuum and air was investigated by means of time-resolved femtosecond diffuse reflectance spectroscopy, and was discussed from the viewpoints of crystal structure (anatase and rutile), particle size, and surrounding condition around the particles. Anatase TiO_2 catalysts showed very rapid (less than 1 ps) and very slow electron−hole recombination processes, while rutile ones did not show any rapid decay. For catalysts composed of small particles, slower electron−hole recombination was observed in air compared with that in a vacuum, which was well explained in terms of upward band bending near the surface due to adsorption of oxygen. The relationship between the observed charge carrier dynamics and photocatalytic reactivity is also discussed.

Introduction

Interfacial photochemical reaction on the surface of TiO_2 particles has attracted much interest because of its potential applications toward photocatalytic reaction of organic molecules, degradation of pollutants, solar energy conversion, and so on.[1−10] Electron or charge-transfer processes between TiO_2 and a molecule adsorbed on the surface are considered to be important in most of the heterogeneous chemical reactions. After band gap excitation of TiO_2, photogenerated electrons and holes migrate to the particle surface, followed by their participation in the electron-transfer reaction with adsorbed molecules. In competition with this process, however, trapping and quenching of the photogenerated carriers by defects and electron−hole recombination should take place in a TiO_2 particle. These are part of the most significant factors influencing the overall efficiency of TiO_2 particles as a photocatalyst. Recent time-resolved absorption measurements on TiO_2 colloidal solutions revealed the kinetics of the electron trapping and the recombination in femtosecond and picosecond regions.[11−16] For example, it was reported that conduction band electrons are trapped at Ti^{4+} centers of the colloid within a few picoseconds after excitation and generate Ti^{3+} species. The trapped electrons give a broad absorption centered around 500−650 nm,[12,17,18] depending on the particle size and other conditions.[11] It was also found that photogenerated electrons are trapped at the surface of TiO_2 nanocrystals within a few 100 fs, and subsequently most of them undergo electron−hole recombination within the first 100 ps, which obeys second-order kinetics.[13,14] In the transient absorption spectral measurements of TiO_2 colloidal solution in the nanosecond to microsecond region, an absorption band centered around 430 nm was ascribed to the absorption of trapped holes and a band centered around 650 nm to trapped electrons.[19−21]

It is known that photocatalytic reactivity strongly depends on the nature of TiO_2 particles,[22] such as crystal structures, particle sizes, defects, and impurities. Since they also affect the charge carrier dynamics, it is necessary to examine ultrafast charge carrier dynamics of TiO_2 particles, which are applied to photocatalytic chemical reactions, and to relate directly the dynamics to their physical and catalytic properties. However, only a few reports address such a viewpoint. This lack is due to the experimental difficulty of optical conditions in measurements on such catalysts. Transmittance-mode transient absorption spectroscopy, which is useful for colloidal solutions, cannot be generally applied to TiO_2 photocatalytic samples in situ, because many of them are opaque light scatterers.

Time-resolved diffuse reflectance spectroscopy,[23−26] where diffuse reflected light is used as monitoring light instead of transmitted light in conventional spectroscopic methods, is very powerful to analyze the dynamics of photoexcited states in optically opaque systems, and it has been applied also to TiO_2 powder.[27−32] Moreover, one of advantages of this spectroscopic technique is that surrounding conditions of particles can be varied widely (gas, liquid, or vacuum). Colombo et al. reported femtosecond diffuse reflectance spectroscopic studies on TiO_2 powder using a CPM dye laser (75 fs pulse width, 310 nm excitation, and 620 nm probe wavelengths).[33,34] However, spectral information on transient species was not available because of the fixed probe wavelength. To measure transient absorption spectra in a wide wavelength region is very useful for assignment of transient species and necessary for discussion of their electronic properties. Recently, we have developed a femtosecond diffuse reflectance spectroscopic system using a femtosecond white continuum as a spectral measurement light source,[35−37] and applied it to an opaque suspension of TiO_2 powder adsorbed with electron acceptor molecules[38] and two standard TiO_2 catalytic powders [JRC-TIO-2 and -4 (generally known as Degussa P-25)].[39]

In the present work we report femtosecond diffuse reflectance spectroscopic studies on five "standard TiO_2 catalysts", JRC-TIO-1, -2, -3, -4, and -5 whose photocatalytic and physical properties were examined. We investigated excitation intensity

* Author to whom correspondence should be addressed.
[†] Osaka University.
[‡] University of Osaka Prefecture.

10.1021/jp984162h CCC: $18.00
Published on Web 04/07/1999

TABLE 1: Summary of Physical Properties and Transient Absorption Spectral Data of "Standard TiO_2 Catalysts"; JRC-TIO-1, -2, -3, -4, and -5

catalysts	crystal[a] structure	particle size (nm)[a,b]	surface area (m^2/g)[a]	decay components	temporal spectral change	environmental effect[d]
JRC-TIO-1	anatase	*	73	~1 ps, const[c]	yes	red-shift
JRC-TIO-2	anatase	400	16	~1 ps, const[c]	yes	no
JRC-TIO-3	rutile	30−50	51	a few 100 ps, const[c]	yes	slow decay
JRC-TIO-4	(mainly) anatase	21	49	a few 100 ps, const[c]	yes	red-shift, slow decay
JRC-TIO-5	rutile	640	3	~10 ns	no	no

*Judging from the surface area, the particle size will be relatively small (roughly a few 10 nm). [a] From ref 45. [b] Primary particle diameter. [c] Almost constant in a nanosecond region. [d] Spectral difference of measurements in air from those in a vacuum.

dependence of the electron−hole recombination kinetics, and effects of the surrounding condition of the particles by measuring their transient absorption spectra in a vacuum and air. The observed charge carrier dynamics depending on the nature of the catalysts will be discussed in terms of the crystal structure, particle size, and photocatalytic reactivity.

Experimental Section

Five kinds of standard TiO_2 catalysts supplied by the Catalysis Society of Japan were examined. Detailed information on these catalysts is available from the Society.[40] Some of their physical properties are listed in Table 1. As a pretreatment for transient absorption measurements, the samples in a quartz cell (2 mm thickness) were heated in pure O_2 at 723 K for 4 h, and degassed to 1×10^{-5} Torr at 473 K for 1 h. After the measurements of these samples, they were exposed to air longer than 1 day and measured again.

Absorption spectra of the ground state are evaluated by the Kubelka−Munk function:

$$\frac{K}{S} = \frac{(1-r)^2}{2r} \qquad (1)$$

where K and S are absorption and scattering coefficients, respectively, and r is diffuse reflectance. We measured here a relative value of r using MgO powder as a reference. Diffuse reflected light intensity was measured by a fluorescence spectrometer (F-4500, HITACHI), scanning wavelengths of incident and detected light synchronously.

The details of a femtosecond diffuse reflectance spectroscopic system have been reported elsewhere.[36] Briefly, a light source consists of a cw self-mode-locked Ti:sapphire laser (Mira 900 Basic, Coherent) pumped by an Ar^+ laser (Innova 310, Coherent) and a Ti:sapphire regenerative amplifier system (TR70, Continuum) with a Q-switched Nd:YAG laser (Surelight I, Continuum). The fundamental output from the regenerative amplifier (780 nm, 3−4 mJ/pulse, 170 fs fwhm, 10 Hz) was frequency doubled (390 nm) and used as an excitation light pulse. The energy of the excitation pulse measured with a Joule meter (P25, Scientech) was several tens μJ and its spot size on the sample was nearly 2 mm. The shot-to-shot fluctuation of the energy was less than ±10%. The residual of the fundamental output was focused into a quartz cell (1 cm path length) containing H_2O to generate a white-light continuum as a probe pulse. Transient absorption intensity was displayed as percentage absorption:[24]

$$\%\ \text{absorption} = 100 \times (1 - R/R_0) \qquad (2)$$

where R and R_0 represent intensity of the diffuse reflected light of the probe pulse with and without excitation, respectively. Typically, the spectral data was averaged over 150 shots of pulses. We have shown that time resolution of our system is less than 1 ps for the powder with a large absorption coefficient at the excitation wavelength such as organic microcrystals, semiconductor powders, and so on.[36]

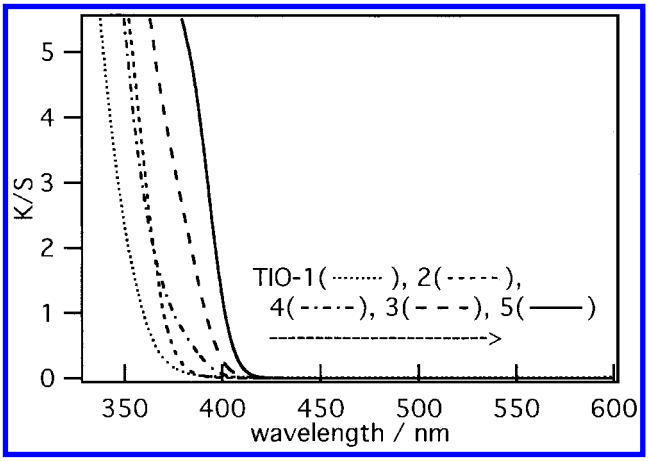

Figure 1. Kubelka−Munk functions of "standard TiO_2 catalysts" (JRC-TIO-1, -2, -3, -4, and -5). K and S are an absorption coefficient and a scattering coefficient, respectively.

Transient absorption spectra of a rutile TiO_2 single crystal (1 mm thickness) in a vacuum were measured with a transmittance-mode femtosecond transient absorption spectroscopic system (400 fs time-resolution), in which transmitted light of the probe pulse through a sample was used for analyzing transient absorption.[41]

Results

Ground-State Absorption Spectra. Figure 1 shows Kubelka−Munk re-emission spectra of the samples in a vacuum. The absorption edge of the samples composed of anatase TiO_2 (TIO-1 and -2) is at a shorter wavelength compared with that of rutile TiO_2 samples (TIO-3 and -5), since anatase TiO_2 has a large band gap compared with that of rutile.[42,43] However, it is reported that the absorption coefficient of anatase TiO_2 at the excitation wavelength (390 nm) is still several tens cm^{-1} at room temperature.[42] Indeed, diffuse absorbance $(1 - r)$ at 390 nm of anatase samples (~20%) responsible to photon absorption was only about four times smaller than that of rutile ones (~80%), although Figure 1 represents a very large difference in their absorption coefficients at the excitation wavelength. Hence, it is reasonable to consider that the present excitation condition corresponds to band gap excitation for all samples. On the other hand, difference in the samples with the same crystal structure can be ascribed to a particle size effect. For a powder sample consisting of small particles, its scattering coefficient S is large, so that K/S (Kubelka−Munk function) becomes smaller than that of the powder sample of large-sized particles with the same absorption coefficient (K). It is noted

that the absorption spectra in air are almost the same as those in a vacuum.

Transient Absorption Spectra. Transient absorption spectra of the standard catalysts in a vacuum and in air are presented in Figure 2. Also, the rise and decay profiles of the transient absorption are summarized in Figure 3. Very broad transient absorption spectra covering the whole visible region are observed for all samples, and they can be ascribed to photogenerated carriers (electrons and/or holes) of these catalysts.[39] The details will be discussed later. Their spectral shapes and temporal profiles depending on the nature of catalysts are clearly observed, and are summarized in Table 1.

Excitation intensity dependence of the decay profiles is shown in Figure 4. In TIO-3, -4, and -5, decays after about 10 ps are faster at higher excitation intensity, which suggests second-order kinetics of electron−hole recombination. Decays of TIO-1 and -2 in the nanosecond region are almost independent of excitation intensity. On the other hand, the fast decay components depend on excitation intensity. When the decay profiles under the two excitation conditions are normalized around 10 ps, it is found that the decay component with almost the same decay rate (about 1 ps) is relatively larger at weaker excitation intensity. In general, when actual decay is faster than the time resolution of the apparatus, observed decay appears as relatively smaller absorption. Hence, it is considered that the decay is faster than 1 ps and second-order electron−hole recombination is involved in the rapid decay components of TIO-1 and -2.

Comparison between in a Vacuum and in Air. We here compare transient absorption spectra (Figure 2) and their decay profiles (Figure 3) between in a vacuum and in air. In air, oxygen and water molecules should be adsorbed on the particle surface and will influence the charge carrier dynamics at and near the surface to some degree. In the case of TIO-1, -3, and -4 whose surface area is larger than that of TIO-2 and -5, spectral shapes and time profiles depend on the experimental condition. Then, it is quite likely that observed dynamics of photogenerated charge carriers of TIO-1, -3, and -4 is ascribed to the processes near or at the surface. It is worth noting that decay of the charge carriers of samples in air is slower than that in a vacuum, which will be discussed later. On the other hand, TIO-2 and -5 do not show any apparent difference in the experimental results under the two conditions, which will be due to a large bulk-to-surface ratio (Table 1).

TiO_2 Single Crystal. As a reference, we have measured transient absorption spectra of a single crystal of rutile TiO_2 by conventional transmittance-mode spectroscopy. As shown in Figure 5, absorption spectra having a broad peak around 700 nm were observed from 0 ps to 6 ns without any appreciable temporal spectral change.

Discussion

Nature of Photogenerated Charge Carriers. As described above, in the colloidal solution of TiO_2 nanoparticles, whose crystal structure is anatase,[44] photogenerated electrons in the conduction band are considered to be trapped in less than a few 100 fs.[13,14] Consequently, the Ti^{3+} species is generated by the electron trapping, giving an absorption band around 500−650 nm.[11,12,17,18] Also, in the nanosecond to microsecond region, absorption spectra centered around 430 and 650 nm were ascribed to trapped holes and electrons, respectively.[19−21] In the rutile TiO_2 single crystal, transient absorption spectra did not change up to 6 ns delay time (Figure 5). The absorption spectrum with its maximum at 700 nm is ascribed to trapped carriers, because charge carriers should be already trapped in a nanosecond region. This fact means photogenerated carriers are trapped less than 400 fs (time resolution of our system) also in rutile TiO_2. Consequently, we attributed the observed transient absorption spectra for the five standard photocatalytic powders to absorption bands of trapped electrons and/or holes. It is likely that absorption in the long wavelength region is ascribed to trapped electrons (Ti^{3+} species).

We here discuss the observed transient absorption spectra in view of crystal structure. TIO-1 and -2, which are composed of anatase, showed similar decay profiles of transient absorption; very fast (∼1 ps) and very slow (>5 ns) decays. These will be characteristic behaviors of anatase crystals including colloidal TiO_2, since TiO_2 powder obtained by precipitation from a colloidal solution also showed similar decay behaviors.[35] The fast and slow decay components may be attributed to electrons trapped at shallow and deep sites, respectively, although detailed physical natures cannot be identified at the present stage of investigation. The slow decay in a nanosecond region is almost independent of the excitation intensity. Then, it is considered that in anatase crystals there are numerous deep trapping sites of electrons. In one of the works on colloidal TiO_2 nanoparticles, photogenerated carriers are considered to be trapped at the surface as Ti^{3+} species.[12] However, our results of the environmental effect indicate that both trapped electrons in bulk and at/near the surface show similar absorption spectra and decay behavior (fast and slow decays).

On the other hand, TIO-3 and -5 are composed of rutile. TIO-5, in which bulk carriers were observed, showed similar transient absorption spectra to those of the single crystal (a peak around 700 nm and slow decay without any spectral change). This spectrum can be regarded as a characteristic feature of trapped electrons in bulk of rutile TiO_2. The peak of transient absorption spectra of TIO-3 is around 700 nm immediately after excitation, and then shifts to a shorter wavelength with time. This will mean that trapped electrons similar to those in the single crystal are generated at first and then migrate and relax to more stable trapping sites that do not exist in the single crystal. They will include trapping sites near the particle surface. As mentioned above, the absorption band of anatase colloids in the short-wavelength region was ascribed to trapped holes.[19−21] One of other possibilities for the temporal peak shift is differing amounts of electrons and holes. However, the peak shifts continuously with time and observed absorption spectra cannot be represented by superposition of two spectral components (electrons and holes). Hence, we consider the observed shifts in absorption to be mainly due to change in the distribution of the various trapped electrons.

Clear dependence of decay profiles on the crystal structure may be partially derived from the excitation condition. Excitation wavelength (390 nm) corresponds to almost the same energy as the band gap energy for anatase TiO_2 and to enough higher energy than that for the rutile one. Therefore, density of charge carriers generated by excitation should be much higher for rutile samples. Ohtani et al. recently reported transient absorption decays at 620 nm of TIO-2 and -4 excited with 310 nm pulse (75 fs).[34] In TIO-4, faster decay than our result was observed; in TIO-2, any rapid decay (∼1 ps) was not observed. One of explanations is high density of photogenerated charge carriers due to a large absorption coefficient at the 310 nm excitation wavelength. Now, we are investigating excitation wavelength dependence and will publish it elsewhere.

TIO-4 is composed of both anatase (70−80%) and rutile (20−30%), though whether individual particles include both crystal phases or one phase still has been ambiguous.[45−47] Despite 70−

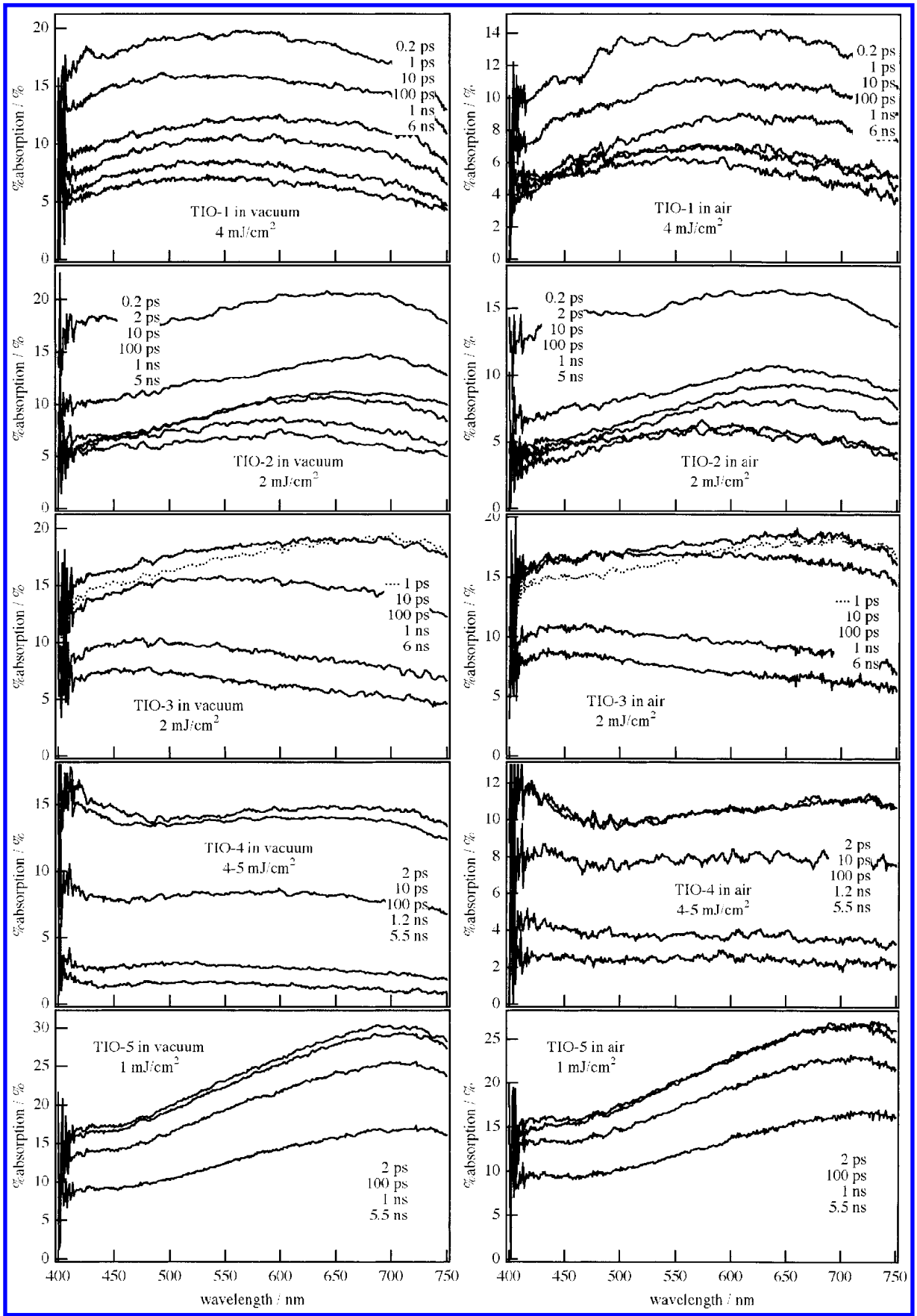

Figure 2. Transient absorption spectra of "standard TiO_2 catalysts" (JRC-TIO-1, -2, -3, -4, and -5) in a vacuum (left-hand) and in air (right-hand) excited by a femtosecond laser pulse (390 nm). Excitation intensity and delay times after the excitation are indicated in each graph. The excitation intensity has an error of almost ±15%.

80% occupancy of anatase, the transient absorption decay of TIO-4 is quite different from those of TIO-1 and -2, and rather similar to that of TIO-3. This suggests that trapped carriers in rutile domains but not in anatase ones are observed. The energy

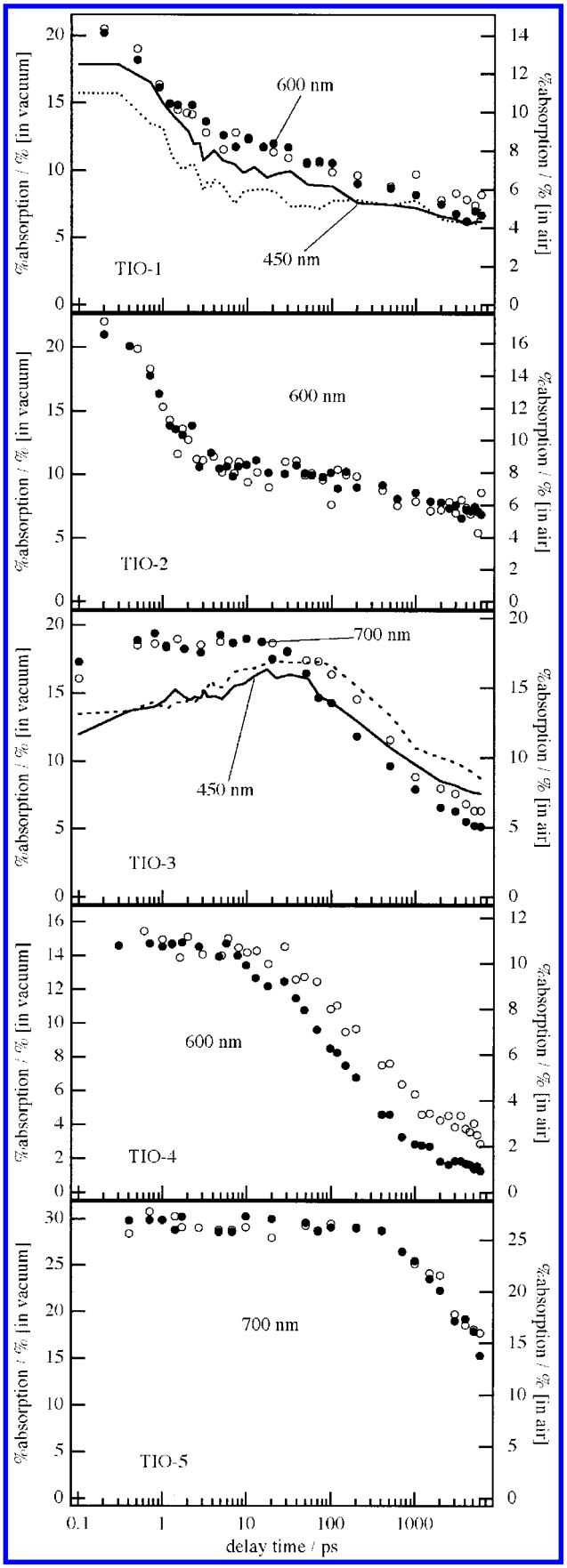

Figure 3. Temporal profiles of the transient absorption of "standard TiO_2 catalysts" (JRC-TIO-1, -2, -3, -4, and -5) in a vacuum (● or solid line) and in air (○ or dashed line) excited by a femtosecond laser pulse (390 nm). Observation wavelength is given in each graph and excitation intensity is the same as the corresponding one in Figure 2.

level of the conduction band of rutile is known to be lower than that of anatase. Hence, photogenerated carriers in anatase domains may migrate quite rapidly (<1 ps) to rutile ones, if anatase and rutile domains coexist in one particle. Another interpretation is that rutile domains are selectively excited under the present experimental condition, because the absorption coefficient of rutile is larger than that of anatase at the excitation wavelength. To clear this problem, a study on the excitation wavelength dependence is now in progress in our laboratory and the results will be published elsewhere.

Recombination Kinetics. The excitation intensity experiments showed second-order kinetics of electron−hole recombination. We here analyze the experimental results of TIO-3, -4, and -5 using the following equation of second-order kinetics with a constant component:

$$\%\ \text{absorption} = \frac{\alpha[C_0]}{k_r[C_0]t + 1} + \text{const} \qquad (3)$$

where $[C_0]$ and k_r refer to initial concentration of photogenerated carriers, and a second-order rate constant for electron−hole recombination, respectively. A coefficient α is dependent on an extinction coefficient of photogenerated carriers and a scattering coefficient of powder.

As shown in Figure 4, for each sample of TIO-3, -4, and -5, temporal profiles by two excitation intensities are well analyzed fixing k_r almost to a certain value and proportional $[C_0]$ to the excitation intensity. To compare the three samples, we here consider α to be same for the three samples, although α is actually unknown and dependent on the sample. Then, ($\alpha[C_0]$ + const) equals % absorption just after excitation. On this assumption, relative values of k_r were estimated to be about 40, 100, and 1 for TIO-3, -4, and -5, respectively. The second-order electron−hole recombination of TIO-3 and -4 are much faster than that of TIO-5. In TIO-3 and -4, carriers trapped at or near the surface are considered to be mainly observed. Actually the trapping sites will be numerous there compared with those in bulk due to lattice disorder and dangling bonds, which will result in an effectively higher density of carriers near the surface and, resultingly, fast recombination. Moreover, some of such trapping sites may act as an efficient electron−hole recombination center.

Effect of Environmental Conditions. From the differences of transient absorption spectra and/or their decay profiles between in a vacuum and in air, we attributed the observed charge carriers of TIO-1, -3, and -4 to those at or near the surface. In air, water and oxygen molecules are considered to be adsorbed on the TiO_2 surface. The charge carriers just at the surface would be quenched by the adsorbed molecules, leading to their faster decay compared with those in a vacuum. However, slower decay in air than in a vacuum was observed. Here we discuss the reason for the slower decay. The effects of adsorption of the molecules onto the surface of TiO_2 (rutile) have been discussed by one of authors (M. Anpo) on the bases of fluorescence quenching measurements.[48] Adsorption of oxygen molecules leads to upward bending of conduction and valence bands near the surface owing to an electric double layer. When charge carriers are generated by photoexcitation, the band bending leads to spatial separation of electrons to the inside and holes to the surface and results in suppression of their recombination. This explains well the slower electron−hole recombination in air. Accordingly, the trapped electrons in the surface neighborhood but not carriers just at the surface are considered to be observed.

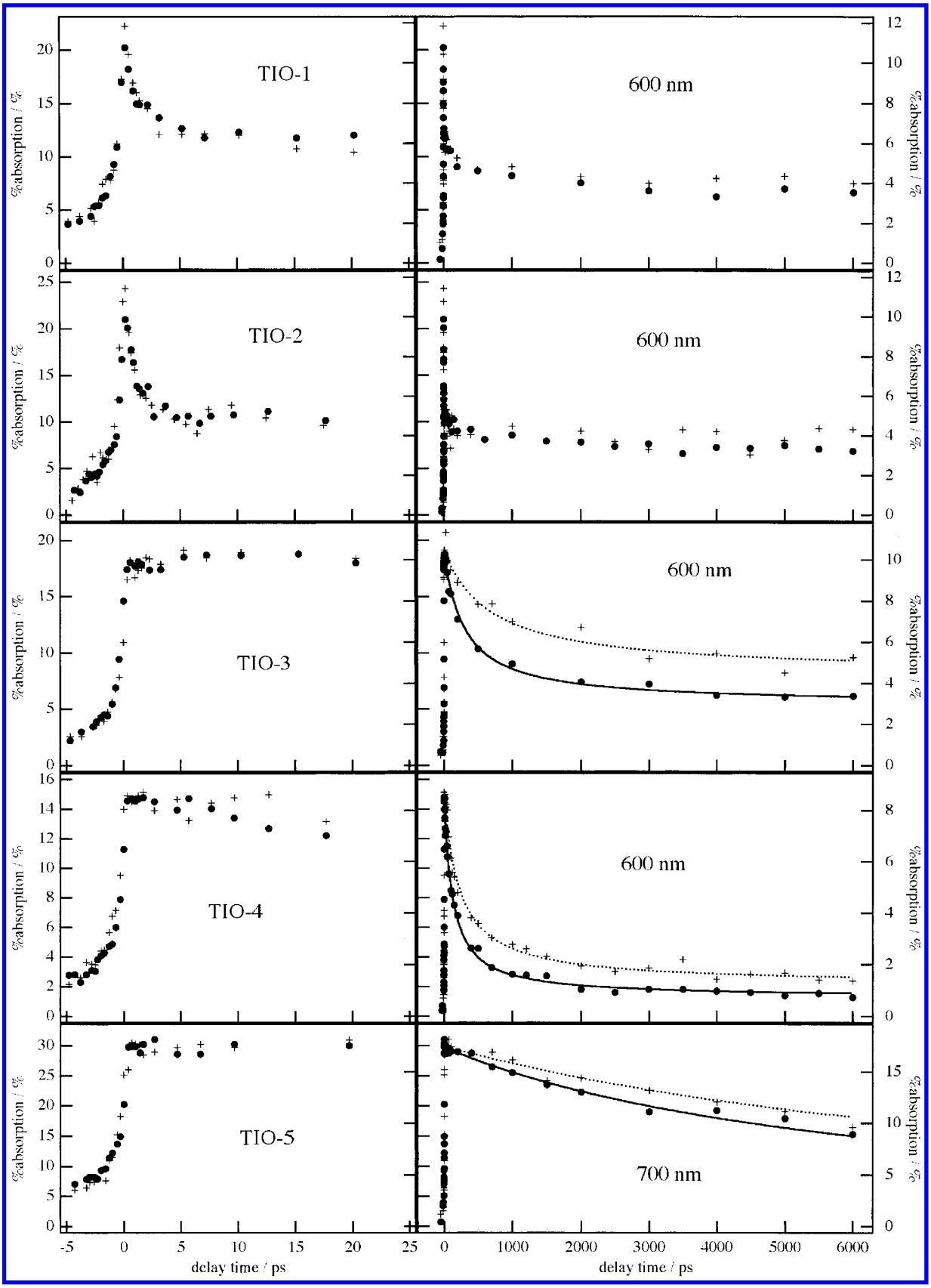

Figure 4. Excitation intensity dependence of the temporal profiles of the transient absorption of "standard TiO_2 catalysts" in a vacuum. ● (left axis) indicate the profiles at the same excitation intensity as in Figure 3. + (right axis) indicate those at the half intensity of ● for each of the samples. Solid or dashed lines are curves based on second-order kinetics.

As described above, temporal peak shifts of transient absorption spectra to short wavelength can be considered to reflect a migration process of trapped carriers from bulk to the surface. The transient absorption spectra of TIO-1 and -4 in air were slightly red-shifted compared with those in a vacuum at the same delay time (Figure 6), which may indicate electrons were

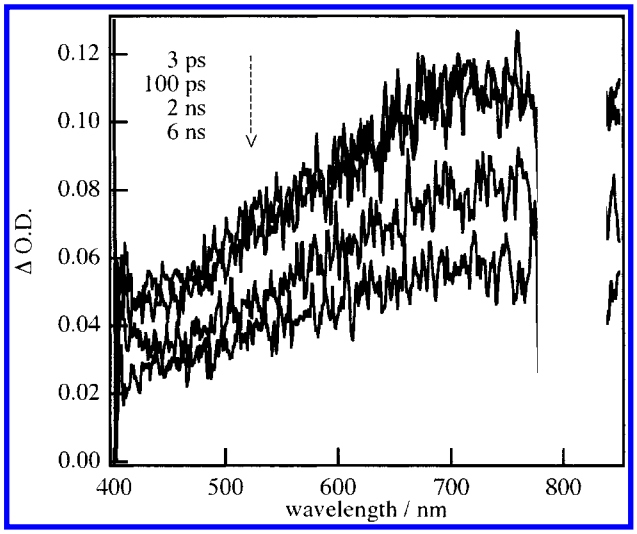

Figure 5. Transient absorption spectra of a rutile TiO_2 single crystal (1 mm thickness) in a vacuum excited by a femtosecond laser pulse (390 nm, ~14 mJ/cm^2).

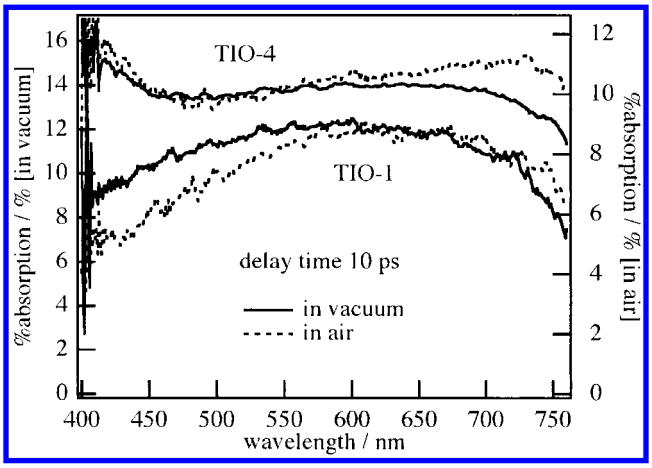

Figure 6. Comparison of transient absorption spectra of TIO-1 and -4 between in a vacuum and in air at 10 ps after excitation.

retained away from the surface by the steeper band bending in air. This is consistent with the above discussion on the charge separation.

Relationship to Catalytic Reactivity. In general, when the photogenerated charge carriers exist near the particle surface and have a long lifetime and the rate of charge transfer to surface molecules is large, high catalytic reactivity will be achieved. We here discuss the above experimental results from the viewpoint of the first two conditions, because the third condition is dependent on energy levels of trapping states of TiO_2 and the redox potential of the surface molecules.

TIO-4 is well-known to have higher photocatalytic reactivity than the others. Also, as one example of investigations on photocatalytic reactivity of TIO-1−5, reactivity of liquid-phase oxidative degradation of 1-octanol under UV light irradiation at 350 nm has been reported as nearly TIO-4 > -3 > -1 > -5 > -2.[22] In this photocatalytic reaction, O_2^- generation by transfer of photogenerated electrons in the TiO_2 band to surface O_2 molecules is considered to be a primary process. Results of the transient absorption measurements have a good correlation with the relative reactivity. Namely, the transient absorption behaviors of catalysts with higher reactivity show spectral and/or decay changes between "in vacuum" and "in air" conditions and do not show any rapid decays (~1 ps). The former indicates most of the trapped electrons exist near the surface (not at the surface, as discussed above) and the latter reflects that shallow trapped carriers immediately after photogeneration can escape from their recombination. Both cases mean existence of the large number of electrons or holes which can contribute to redox reactions. It should be noted that recombination processes observed in 100 ps range for the samples TIO-3 and -4 do not occur under usual weaker excitation conditions in the experiments of photocatalytic reactions. Existence of numerous photogenerated carriers usable for redox reaction is above all very important for higher photocatalytic reactivity, though other factors, such as lifetimes of nano- and microsecond region, rates of interfacial charge transfer, and so on, are related.

Summary

The trapping and recombination dynamics of charge carriers generated by UV (390 nm) pulse excitation in five standard TiO_2 catalytic powders was investigated by transient absorption spectral measurements by means of femtosecond diffuse reflectance spectroscopy. Very broad spectra covering the visible region were ascribed to trapped electrons and/or holes. Anatase TiO_2 showed decay components with lifetimes of about 1 ps and more than several nanoseconds. Rutile TiO_2 did not show such a fast decay component. Comparing the results of transient absorption measurements of the samples in a vacuum and in air, it is clearly confirmed that trapped carriers near the surface are relatively numerous in the catalytic powders of small particles. Slower recombination processes in air compared with in a vacuum were ascribed to enhanced upward band bending near the TiO_2 surface due to oxygen adsorption.

As a result of the transient absorption spectral measurements, a good correlation between charge carrier dynamics in TiO_2 particles and photocatalytic reactivity of the oxidative degradation of 1-octanol was found for the five catalysts. Namely, in catalysts with high photocatalytic reactivity, observed trapped carriers mainly exist near the particle surface and do not undergo rapid (~1 ps) recombination immediately after photoexcitation.

References and Notes

(1) Kamat, P. V. *Chem. Rev.* **1993**, *93*, 267.
(2) Fox, M. A.; Dulay, M. T. *Chem. Rev.* **1993**, *93*, 341.
(3) Hagfeldt, A.; Grätzel, M. *Chem. Rev.* **1995**, *95*, 49.
(4) Hoffmann, M. R.; Martin, S. T.; Choi, W.; Bahnemann, D. W. *Chem. Rev.* **1995**, *95*, 69.
(5) Linsebigler, A. L.; Lu, G.; Yates, J. T., Jr. *Chem. Rev.* **1995**, *95*, 735.
(6) Mills, A.; Hunte, S. L. *J. Photochem. Photobiol. A: Chem.* **1998**, *108*, 1.
(7) Martini, I.; Hodak, J.; Hartland, G. V.; Kamat, P. V. *J. Chem. Phys.* **1997**, *107*, 8064.
(8) Sahyun, M. R. V.; Serpone, N. *Langmuir* **1997**, *13*, 5082.
(9) He, J.; Zhao, J.; Shen, T.; Hidaka, H.; Serpone, N. *J. Phys. Chem. B* **1997**, *101*, 9027.
(10) Cherepy, N. J.; Smestad, G. P.; Grätzel, M.; Zhang, J. Z. *J. Phys. Chem. B* **1997**, *101*, 9342.
(11) Serpone, N.; Lawless, D.; Khairutdinov, R.; Pelizzetti, E. *J. Phys. Chem.* **1995**, *99*, 16655.
(12) Rothenberger, G.; Moser, J.; Grätzel, M.; Serpone, N.; Sharma, D. K. *J. Am. Chem. Soc.* **1985**, *107*, 8054.
(13) Colombo, D. P. Jr.; Roussel, K. A.; Saeh, J.; Skinner, D. E.; Cavaleri, J. J.; Bowman, R. M. *Chem. Phys. Lett.* **1995**, *232*, 207.
(14) Skinner, D. E.; Colombo, D. P., Jr.; Cavaleri, J. J.; Bowman, R. M. *J. Phys. Chem.* **1995**, *99*, 7853.
(15) Kamat, P. V.; Fox, M. A. *Chem. Lett.* **1983**, *102*, 379.
(16) Gopidas, K. R.; Bohorquez, M.; Kamat, P. V. *J. Phys. Chem.* **1990**, *94*, 6435.
(17) Howe, R. F.; Grätzel, M. *J. Phys. Chem.* **1985**, *89*, 4495.
(18) Howe, R. F.; Grätzel, M. *J. Phys. Chem.* **1987**, *91*, 3906.
(19) Bahnemann, D. W.; Hilgendorff, M.; Menning, R. *J. Phys. Chem. B* **1997**, *101*, 4265.
(20) Bahnemann, D.; Henglein, A.; Lilie, A.; Spanhel, L. *J. Phys. Chem.* **1984**, *88*, 709.

(21) Bahnemann, D.; Henglein, A.; Spanhel, L. *Faraday Discuss. Chem. Soc.* **1984**, *78*, 151.
(22) Yamashita, H.; Ichihashi, Y.; Harada, M.; Stewart, G.; Fox, M. A.; Anpo, M. *J. Catal.* **1996**, *158*, 97.
(23) Kessler, R. W.; Wilkinson, F. *J. Chem. Soc., Faraday Trans. 1* **1981**, *77*, 309.
(24) Kessler, R. W.; Krabichler, G.; Uhl, S.; Oelkrug, D.; Hagan, W. P.; Hyslop, J.; Wilkinson, F. *Opt. Acta* **1983**, *30*, 1099.
(25) Zhang, G.; Thomas, J. K.; Eremenko, A.; Kikteva, T.; Wilkinson, F. *J. Phys. Chem. B* **1997**, *101*, 8569.
(26) Worrall, D. R.; Williams, S. L.; Wilkinson, F. *J. Phys. Chem. A* **1998**, *102*, 5484.
(27) Wilkinson, F.; Willsher, C. *J. Chem. Soc., Chem. Commun.* **1985**, 142.
(28) Kamat, P. V.; Gopidas, K. R.; Weir, D. *Chem. Phys. Lett.* **1988**, *149*, 491.
(29) Draper, R. B.; Fox, M. A. *J. Phys. Chem.* **1990**, *94*, 4628.
(30) Nasr, C.; Vinodgopal, K.; Fisher, L.; Hotchandani, S.; Chattopadhyay, A. K.; Kamat, P. V. *J. Phys. Chem.* **1996**, *100*, 8436.
(31) Ziolkowski, L.; Vinodgopal, K.; Kamat, P. V. *Langmuir* **1997**, *13*, 3124.
(32) Kamat, P. V.; Gevaert, M.; Vinodgopal, K. *J. Phys. Chem. B* **1997**, *101*, 4422.
(33) (a) Colombo, D. P., Jr.; Bowman, R. M. *J. Phys. Chem.* **1996**, *100*, 18445. (b) Colombo, D. P., Jr.; Bowman, R. M. *J. Phys. Chem.* **1995**, *99*, 11752.
(34) Ohtani, B.; Bowman, R. M.; Colombo, D. P. Jr.; Kominami, H.; Noguchi, H.; Uosaki, K. *Chem. Lett.* **1998**, 579.
(35) Asahi, T.; Matsuo, Y.; Masuhara, H. *Chem. Phys. Lett.* **1996**, *256*, 525.
(36) Asahi, T.; Furube, A.; Fukumura, H.; Ichikawa, M.; Masuhara, H. *Rev. Sci. Instrum.* **1998**, *69*, 361.
(37) Asahi, T.; Furube, A.; Masuhara, H. *Bull. Chem. Soc. Jpn.* **1998**, *71*, 1277.
(38) Asahi, T.; Furube, A.; Masuhara, H. *Chem. Phys. Lett.* **1997**, *275*, 234.
(39) Furube, A.; Asahi, T.; Masuhara, H.; Yamashita, H.; Anpo, M. *Chem. Lett.* **1997**, 735.
(40) Murakami, Y. In *Preparation Catalysts III*; Catalysis Society of Japan: Tokyo, 1983; p 775.
(41) Watanabe, K.; Asahi, T.; Fukumura, H.; Masuhara, H.; Hamano, K.; Kurata, T. *J. Phys. Chem. B* **1997**, *101*, 1510.
(42) Tang, H.; Lévy, F.; Berger, H.; Schmid, P. E. *Phys. Rev. B* **1995**, *52*, 7771.
(43) Tang, H.; Berger, H.; Schmid, P. E.; Lévy, F. *Solid State Commun.* **1994**, *92*, 267.
(44) O'Regan, B.; Moser, J.; Anderson, M.; Grätzel, M. *J. Phys. Chem.* **1990**, *94*, 8720.
(45) In *Databook of standard catalysts of the Catalysis Society of Japan*; Catalysis Society of Japan: Tokyo, 1986.
(46) Bickley, R. I.; Gonzalez-Carreno, T.; Lees, J. S.; Palmisano, L.; Tilley, R. J. D. *J. Solid State Chem.* **1991**, *92*, 178.
(47) Datye, A. K.; Riegel, G.; Bolton, J. R.; Huang, M.; Prairie, M. R. *J. Solid State Chem.* **1995**, *115*, 236.
(48) Anpo, M.; Chiba, K.; Tomonari, M.; Coluccia, S.; Che, M.; Fox, M. A. *Bull. Chem. Soc. Jpn.* **1991**, *64*, 543.